Paleoearthquakes of the Düzce fault (North Anatolian Fault Zone): implications for earthquake recurrence

Pantosti, D. [a, *], **S. Pucci** [a,b], **N. Palyvos** [a], **P.M. De Martini** [a], **G. D'Addezio** [a], **P. E.F. Collins** [c,] **C. Zabci**[d]

[a] *Istituto Nazionale di Geofisica e Vulcanologia, Via di Vigna Murata 605, 00143 Rome, Italy*

[b] *Dipartimento di Scienze della Terra, Università degli studi di Perugia,Piazza Università, 06123 Perugia, Italy*

[c] *Geography & Earth Sciences, Brunel University, Uxbridge UB8 3PH, UK*

[d] *ITU Istanbul, Turkey*

* Corresponding author. Current address: *Istituto Nazionale di Geofisica e Vulcanologia, Via di Vigna Murata 605, 00143 Rome, Italy* , Tel.: +39-6-51860483, Fax: +39-6-51860507.

E-mail address: pantosti@ingv.it (D. Pantosti).

Abstract

The November 12, 1999, Mw 7.1 earthquake, ruptured the Düzce segment of the North Anatolian Fault Zone and produced ca. 40 km-long surface ruptures.

To learn about recurrence of large surface faulting earthquakes on this fault, we undertook paleoseismological trench investigations. We found evidence for repeated surface faulting paleoearthquakes pre-dating the 1999 event. Dating was based on radiocarbon and ^{210}Pb analyses as well as on archaeological considerations. By merging information obtained from all the trenches we reconstructed the seismic history of the Düzce fault for the past millennium. We correlated coeval events between different trench sites under the assumption that, similarly to the 1999 event, paleoearthquakes ruptured the whole Düzce fault. Besides the 1999 earthquake, prior surface faulting earthquakes are dated as follows: AD1685-1900 (possibly end of 19th century); AD1685-1900 (possibly close to AD 1700); AD1185-1640; AD685-1220 (possibly AD800-1000). Thus, the AD1719, AD1878 and AD1894 historical earthquakes, may have ruptured the Düzce fault and not the faults they are usually associated to or, alternatively, a cascade of events occurred on the Düzce and nearby faults (similarly to the Izmit and Düzce 1999 earthquakes).

Five events since AD 685-1220 (possibly AD800-1000), would yield an average recurrence time for the Düzce fault, of 200-325 yr (possibly 250-300 yr). The three most recent earthquakes, including 1999, occurred within 300 yr and may be suggestive of clustering. Assuming that the average 1999 slip is characteristic for this fault, the above recurrence times yield slip rates of 6.7-13.5 mm/yr.

1. Introduction

The November, 12, 1999, Mw 7.1 earthquake ruptured the Düzce fault segment of the North Anatolian Fault Zone (NAFZ, fig. 1A) producing a ca. 40 km long surface rupture with up to 5 m right-lateral offset (2.7 m average) and up to 2.5 m vertical throws (Akyuz et al., 2000 and 2002; Pucci et al., *submitted*). This earthquake is considered to have been triggered by the Mw 7.4 Izmit earthquake that occurred 3 months earlier (August 17) on the fault segment to the W of the Düzce one.

At a regional scale, the Düzce fault is located just west of the Bolu basin, where the NAFZ starts splaying into two main strands, the Düzce/Karadere to the north and the Mudurnu to the south, to splay again into three major strands in the Marmara Sea (NNAF, CNAF and SNAF in fig.1A, Wong et al., 1995; Armijo et al., 1999; Okay et al., 1999). The Düzce/Karadere strand, together with the Mudurnu fault to its S, accommodate most of the 2-3 cm/yr present-day strain of the NAFZ (Straub et al., 1997; Reilinger et al. 1997 and 2000; Ayhan et al., 1999 and 2001). The Mudurnu segment ruptured entirely during the 1957 and 1967 earthquakes, whereas high seismic potential of the Düzce fault was recognized well before 1999 by Barka and Erdik (1993) that considered this fault the possible source of a near-future earthquake. The Düzce fault has an average E-W trend and a clear geomorphic expression, being the boundary between the Quaternary Düzce and Kaynasli basins to the north and the Paleozoic-Eocene rocks of the Almacik block to the south (fig. 1B). The eastern and western boundaries of the 1999 earthquake rupture appear to be structurally controlled. To the west, the ca. E-W Düzce fault forms a releasing fault junction (*sensu* Christie-Blick and Biddle, 1985) with the NE-SW trending Karadere section (Pucci et al. *submitted*), which ruptured during the Izmit earthquake. To the east, the Düzce fault joins the eastern

single trace of the NAFZ *via* a ca 10-15 km-wide, right-releasing step-over involving the WNW-ESE trending Bakacak and Elmalik faults (fig. 1A) (Barka and Erdik, 1993; Altunel et al., 2000; Barka et al., 2001; Hitchcock et al., 2003). Both these step-overs appear unfavourable to rupture propagation and possibly represent persistent barriers to earthquake ruptures.

Although Turkey has one of the richer records of historical seismicity in the Mediterranean, no clear evidence for historical earthquakes produced by the Düzce segment of the NAFZ during the past centuries has been found. This is probably due to the scarce density of population and lack of cultural settlements in historical times in the Düzce region. The only historical earthquakes that are known to be close enough to be potentially associated to the Düzce fault are: AD967, AD1719, AD1754, AD1878, AD1894, and (Ambraseys and Finkel, 1995; Ambraseys, 2002) (fig.1A). Interestingly, local people living near the eastern part of the Düzce fault recall their grandparents telling them about an earthquake at the end of the 19th century, producing ground ruptures exactly where these occurred in 1999.

Because historical information is very limited, knowledge about recurrence of large earthquakes on the Düzce fault can be derived only from paleoseismology. Soon after the 1999 earthquakes several paleoseismological investigations were carried out at different locations along the fault (fig 1B). On the basis of trenching Hitchcock et al (2003) find evidence for three to five paleoearthquakes in the past 2100 years, with a recurrence interval ranging from 300 to 800 years and the penultimate event occurred about 300 years ago. Komut (2005) recognized 6 paleoevents since BC1750 with the one prior to 1999 occurring during the past 500 yr. Emre et al. (2001, 2003a and 2003b) found evidence for three paleoearthquakes since AD665, the oldest and the youngest of which are dated AD665-1050 and AD1650-1750, respectively. Finally, by

paleoseismological geo-slicing and coring investigations, Sugai et al. (2001) developed a surface faulting history for the past 2 millennia at a site in the western part of the fault. Here, these authors recognize four possible/probable paleoearthquakes preceding 1999 and suggest an average recurrence time of 4-500 yr.

In this paper we present the results of trenching at five sites performed during the E.U. project RELIEF, we compare them with results from previous studies, and discuss their implications for the seismic behaviour of the Düzce segment of the NAFZ.

2. Trenching the Düzce fault

We excavated a total of 10 trenches, 7 across the fault and 3 fault-parallel ones, at five different sites along the Düzce fault (Fig. 1B). High water table and the lack of sites with slow and continuous sedimentation made the site selection and trench interpretation problematic. Because of the type of sediments and sedimentary structures crossed, no piercing points to measure individual or cumulative horizontal coseismic offset were found. Dating of paleoearthquakes was based both on radiocarbon and ^{210}Pb analyses. Both dating methods contain large uncertainties. Samples for radiocarbon dating were quite small with high possibility of reworking. Moreover, most of the trenched deposits appear to be younger than 300 yr. The past 300 yr are a very problematic time interval for radiocarbon dating because of the "radiocarbon plateau" produced by fossil fuel combustion (Suess effect, Bradley, 1985) and increasing solar activity following the Maunder minimum (Stuiver and Quay, 1980). As a consequence of this, a precise age cannot be determined because measured radiocarbon ages in the

plateau calibrate with almost equal probability to any age within it. For this reason we limited the number of samples for ^{14}C dating

In this work we also experimented with the use of ^{210}Pb analyses for dating colluvial and marsh deposits, following the sample preparation method used in Cundy et al. (1998). ^{210}Pb derives from the decay of ^{222}Rn, dating is based on the assumption that all the main sources for ^{210}Pb (in situ, from the atmosphere, and from eroded material in the catchment) can be considered constant through time. If this is true, a near-exponential decline of activity with depth would be expected. Previous work by Cundy and Stewart (2004) highlighted the difficulty of developing a precise geochronology based on short-lived radionuclides in depositional settings where sediment texture is very variable and deposition has occurred in pulses. It is possible, however, to derive an outline chronology, and to use variations in the ^{210}Pb activity to help identify episodes during which older material was being remobilised in the local sedimentary environment and delivered to the sampling site.

2.1 The Kaynasli trench (KAY)

This trench was excavated across the 1999 ruptures in the floodplain of the Asarsu river (KAY, fig. 1B) at the western edge of a sag pond that is artificially drained by a nearby man-made channel. In this area the dextral and vertical offsets of the 1999 ruptures were 0.7-1.7m and 0.3m, respectively (Akyüz et al., 2000 and 2002; Pucci et al., *submitted*). The trench was about 18 m long and 2 m deep and exposed a sequence of predominantly fine sediments (silt and clay), with intercalated layers of sand and pebbles. Fluvial gravel was exposed at the bottom of the central part of the trench. A description of all stratigraphic units is given in fig. 2. Four charcoal samples were AMS

dated from units *d*, *e*, *f*, and *g* (samples KW-45, KW-02, KW-20, KE-08, see table 1 and fig. 2). They yielded ages ranging from modern to AD 685-890.

Two main fault zones were exposed on both walls of the trench (1 and 2 in Figure 2A and B). They were composed of several splays, most of which ruptured in 1999. A third fault zone (3 in Figure 2A), that was not activated in 1999 was located in the southern part of the trench and it is also highlighted by a sharp change in color of units h and g, possibly because of preferential water circulation in the fracture zone..

In **1999** the rupture reached the surface along at least one of the main branches fault zones 1 and 2 and was subsequently sealed by the post-event unit *b* in fault zone 1. During this event, clay and fine sand were injected along the rupture (fault zone 1, west wall, unit *z*) and at the *c/e* and *d/e* contacts. On the basis of stratigraphic and structural relations, we find evidence for three surface faulting paleoearthquakes before 1999 (Kay2 to Kay4 in the following and in fig. 2). Evidence for the penultimate earthquake, **Kay2**, are fault terminations below unit *d* as well as the presence in both fault zones of large cobbles and small boulders (unit *k*) completely unrelated to the surrounding stratigraphy and buried by unit *d* (see also figs. 2C and D). These cobbles are interpreted as man-made fill of ground fissures formed during an earthquake rupture along which water is flowing, as indicated by alteration coatings on the cobbles and boulders of the unit *k* and by the presence of laminated fine sediment at the base of channel-like features. The pre-penultimate event, **Kay3**, was recognized only in fault zone 1 of the western wall, where two fault splays deformed the trenched sequence up to unit f and the base of unit e. The top part of unit e has not been affected. Thus, we place the event horizon somewhere near the base of unit e.

Evidence for an older event, **Kay4**, was found at fault zones 2 and 3. On the western wall, the northern strand of fault zone 2 offset only *g* and older units.

Similar features define Kay4 also in fault zone 3.

On the basis of the dated samples, the timing of the above paleoearthquakes can be constrained as follows: Kay2 is younger than AD1475, Kay3 occurred between AD1035 and 1640, and Kay4 between AD685 and 1220.

2.2 The Mengencik trench site

A total of six trenches were excavated at this site (fig.3) across the 1999 ruptures that attained ca. 3.7m dextral and 0.4m vertical offset (Akyuz et al., 2000 and 2002; Pucci et al., *submitted*). Five of the trenches were located in the western part of the site and one in the eastern. In the following we present results only from the across-fault trenches (Men1, Men5 and Men6, fig. 3B) because observations in the fault-parallel ones were inconclusive.

2.2.1 The western trenches Men1 and Men5

The 1999 earthquake surface fault at the western part of the Mengencik site crosses slope-wash deposits and small coalescent fans composed mainly of silt. Overall, the fault trace produces relative subsidence of the southern side, where ponding is observed against the scarp, especially where the rupture forms small grabens. Repetition of surface faulting events produced the formation of fault-parallel ridges of different size, which clearly control the drainage pattern (fig. 3).

Trench Men1 was excavated across the 1999 ruptures (fig. 4 A, B) where they exhibit an apparent reverse component. The trench exposed a monotonous fan aggradation sequence of silt, fine sand and clay with rare gravel intercalations, derived from the marly deposits forming the range located to the south of the site (see fig. 4 for

description of stratigraphic units). Some layers were rich in organic matter, possibly due to periods of surface stability (soil formation) or ponding events related to pre-1999 surface ruptures (judging from the fact that ponding occurred at this site after the 1999 earthquake). Trench Men5 was excavated about 25 m east of trench Men1 (fig. 3), where the 1999 ruptures formed a graben 1 to 2 m-wide. Similarly to Men1 it exposed a monotonous fan aggradation sequence (fig. 5). Most of the stratigraphy can be directly correlated to that of trench Men1 and, in fact, the same labelling was used for the upper correlative layers. In both trenches the fault zone was about 2 m wide and consisted of several splays in an arrangement that reflects the type of structure observed at the surface: positive flower structure at Men1 and negative at Men5 (figs. 4 and 5). Most of the splays were reaching the surface, indicating that they ruptured also during the 1999 earthquake. Only fault splay B in Men 1 (fig.4 A and C) did not rupture in 1999 and thus it provides good evidence for a previous surface faulting event.

To provide a timeframe to the trenched sediments, we collected samples for ^{14}C, and ^{210}Pb analyses. Radiocarbon dating was quite difficult because of the extremely small size of the available samples and important weathering and reworking. The dated samples (see Table 1 and Figs. 4 and 5) suggest that the upper 60-70 cm of sediments in the southern part of both trenches were deposited maximum during the past ca. 500 yr (samples Men1-W21 and Men5-W20) with the upper 40 cm being younger than AD1700 (possibly AD1880 - 60%probability, sample Men1-W23). Sample Men5-W16 from the bottom of the sediments that were trapped in the shear zone indicates that these are ca. 800 yr old. One further sample dated from unit *d* of trench Men5 (Men5-W13) yielded an out of sequence age indicating occurrence of reworking of material in this environment.

^{210}Pb analysis was completed on the sequence to assess the validity of the radiocarbon chronology and to better constrain the age of the younger part of the stratigraphy in trench Men1. Sampling was performed in the southern part of the trench, from the surface to the bottom of the trench (fig. 4A); analyses were performed for the upper 1.24 m. ^{210}Pb activity shows a general decline with depth (column 1 in fig. 4D). ^{210}Pb activity is noticeably higher in the top 40 cm of the sediment sequence than lower in the sequence. This corresponds mainly to sediments that have buried a paleosol (unit e in fig. 4). Activity levels below this are low, with a slight increase with depth, suggesting in situ production. It is possible to generate ^{210}Pb age estimates for the upper 40 cm using the constant rate of supply model (CRS; Appleby 2001). However, the variable activity levels mean that any derived chronology must be considered with caution. Low activity levels are associated with increased sand content, and probably reflect higher energy episodes on the fan surface. With this caveat, it is still possible to produce an outline chronology (column 2 in fig. 4D) which suggests that the upper 40cm accumulated since the mid 20th Century. Re-running the model with high and low values omitted suggests sediment from 40cm depth was deposited since AD1940-1960. This gives an average accumulation rate of around 0.75 cm a^{-1}, with the highest rates (c. 1.5 cm a^{-1}) possibly occurring since ca. AD1986.

The stratigraphic unit at 40cm depth (unit *e* in fig. 4), which exhibits very low ^{210}Pb activity, is characterised by a blocky ped stuctures and is interpreted as a probable paleosol.^{210}Pb activity increases below the paleosol, probably reflecting *in situ* ^{210}Pb production. A single ^{14}C date of AD1450-1630 (sample Men1-W21) from below the palaeosol supports the hypothesis that this soil represented a phase of relative surface stability and pedogenesis between the 17th-19th Centuries. Similarly, a ^{14}C date from immediately above the palaeosol yields a modern age, possibly younger than AD1880

(sample Men1-W23), supporting the conclusion of the ^{210}Pb analysis. A small piece of aluminium foil, found within unit b, is also supportive of the youthfulness of these upper units.

At the site of trench Men1 the **1999 earthquake** formed a gentle south-facing scarp, with the ruptures clearly reaching the surface at fault zones A and C. Evidence for at least 2 paleoearthquakes predating 1999 was found on the basis of stratigraphic and structural relations at both trenches (figs. 4A and 5B).

The **penultimate earthquake, Men1-2**, was associated with intense deformation at fault zone B, where the grey organic silt units *e*, *f* and *d* (and *k*?) were taken into the fault zone, sheared, and buried by the yellow silt and clay and the organic grey silt layers of units *b* and *c*. A **third event**, **Men1-3**, can be inferred on the basis of the presence and geometry of the grey organic silt units *f* and *e*, which are interpreted as post-earthquake ponding deposits that accumulated inside a depression in front of a coseismic scarp, similar to the one formed by the 1999 earthquake. Structural evidence for this paleoearthquake can be derived from the upper termination of the southern branch of fault zone B (U in fig. 4A) below unit *f*. A thin fissure (F in fig. 4A) located in the northern splay of fault zone B, filled by unit *e*, can be interpreted as further evidence of this earthquake. However, we cannot exclude the possibility that this may not be a fissure predating the deposition of unit *e*, but a slice of this unit trapped between fault splays during the penultimate event. At trench Men5 the **1999 earthquake** ruptures produced a graben-like structure at the surface (negative flower structure), with the free faces still clearly visible in 2004 (fig. 5). The determination of the **penultimate event**, **Men5-2**, is based only on the assumption that, similarly to what was observed after the 1999 earthquake, surface faulting earthquakes at this location produce fault-controlled ponding. On this basis and because of the peculiar thickening of the comparatively

organic-rich unit *ee* towards the fault zone, we assume that this unit deposited in a depression created by surface faulting, thus, it buried (post-dates) an event horizon (Men5-2). Older events, **Men5-old,** have produced intense shearing and slicing of the sediments, accompanied by deposition of organic-rich silt and sand within fault-controlled ponds in the fault zone.

On the basis of the available dating, we can conclude that the penultimate earthquake at the western trenches of Mengencik site (Men1 and Men5) is recognized only in Men1 and post-dates the deposition of unit *d*): thus, occurred after the development of the pedogenic layer e. According to radiocarbon dating (Men1-W23) this event is younger than AD1700, with a ca. 60% probability of being younger than 1880. Although with uncertainties, ^{210}Pb modeling suggests that this event occurred in recent times, possibly close to 1900. Paleoearthquake Men1-3 has a perfect stratigraphic and age correspondence with Men5-2 and is expected to have occurred sometime in the past ca. 500 yr. It is clear that records for more events in the trenched deposits exist but, we were not able to decipher them. The age of possible earthquake-related ponding sediments trapped at the bottom of the fault zone of Men5 (unit *z*) are suggestive of an event that occurred after AD1185 (Men5-W16) and before 1655 (Men5-W20).

2.2.2 The eastern trench: Men6

Trench Men6 was opened about 200 m east of the western trenches (Men1 and Men5) where the 1999 earthquake surface ruptures were distributed in two zones spaced ca. 12 m apart, forming a graben filled by silty slope-wash deposits and hosting ephemeral drainage (fig. 3). The coseismic graben structure coincides with a larger

morphological depression, which indicates that the same pattern of surface ruptures has repeated in the past at this location.

The sediments exposed in the trench walls form a monotonous alluvial fan aggradation sequence of silt, fine sand and clay with rare gravel intercalations (see fig. 6 for description of stratigraphic units). Deposition occurred in pulses, with possible changes of energy conditions through time. The organic component becomes important in the southern part of the trench, probably related to localised formation of a small marsh. The fault zone bounding the graben to the north was composed by several, sub-parallel, south-dipping splays that reach the surface or the ploughed layer. Here, the stratigraphy was unfortunately very homogeneous and contained too many ambiguities to be of use for individual paleoearthquakes recognition. Conversely, the southern fault zone is more complex and is composed by several splays, some of which bounding the main graben (E and D) and others (B and C), forming a small secondary graben (fig. 6).

In order to provide a chronology of the exposed sediments, we collected several charcoal samples for ^{14}C analyses. Also in this trench the charcoal samples are very small and experienced important reworking and weathering, thus dating was quite problematic. Four of these samples were dated (see Table 1 and fig. 6). One of them is modern (sample MAN6-W18). Three others have overlapping ages younger than ca. AD1650 (samples MAN6-W11, MAN6-E35, MAN6-E37). As a whole, we can conclude that the deposits filling the small secondary graben of the southern fault zone (units above *n*) are younger than AD 1685 (fig. 5).

The **1999 earthquake** ruptures produced slip mainly on faults E, D and C of the southern fault zone with a clear down-to-the-north vertical component, indicated by free faces still visible at the surface. Paleoearthquake evidence is derived from stratigraphic and structural relations at the southern fault zone, where we found evidence for at least

two paleoearthquakes pre-dating 1999 (fig. 6). Evidence of the **penultimate event Men6-2** is clear on both trench walls. On the W wall (fig 6D) it is defined by a small graben between faults A and C, with faults sealed by the yellow silt of unit *e* filling it. On the E wall (fig. 6C) the event horizon is defined on the basis of: (1) faulting of a burn layer (unit *f*), successive backward erosion of the free-face and filling of a depression by unit *e*; (2) upward fault terminations at the top of unit *i*; (3) possible paleo-liquefactions within layer *g*. Thus, the event horizon for **Men6-2** is set at the base of unit *e*. Recognition of a further event **(Men6-3)** is based on upward terminations of fault B sealed by unit *n* at both walls and of fault zone E under unit *u* on the east wall. Also, the fact that unit *n* is organic-rich, in striking contrast to the surrounding units (*r* and *s*), may suggest that it was deposited in a fault-controlled depression with marsh vegetation.

With the presently available radiocarbon ages, we can only conclude that events MAN6-2 occurred within the past ca. 300 yr whereas MAN6-3 occurred close to or just before AD 1685 (because it triggered the formation of the pond containing the dated samples).

2.3 The Cakir Haci Ibrahim trench (CH)

The *Cakir Haci Ibrahim* trench was excavated in the floodplain of the Develi River, across a gentle and broad cumulative south-facing scarp (figs. 1B and 7). In this area, the 1999 ruptures formed a ca.100 m wide left step-over and similar but smaller-scale left-stepping scarplets formed exactly at the trench location (fig. 7). At this site the 1999 earthquake dextral and vertical offsets amounted to ca. 3.8m and 1.0m, respectively (Akyuz et al., 2000 and 2002; Pucci et al., *submitted*). Because of their geometry and kinematics, the 1999 ruptures completely dammed an artificial channel

probably built along a natural drainage flowing S to N from the range toward the Develi river (figs. 1B and 7A).

The trench exposed 5 fault zones, distributed within ca. 20 m, displacing gravel-dominated alluvial plain deposits, including layers of sand and silt (see fig. 7D for description of stratigraphic units in the main fault zone). The main of these fault zones A and B are associated with the main flexural scarp, whereas the others with minor scarps (not included in the log of fig. 7D).

In order to provide chronological constraints for the trench deposits, charcoal and wood samples were collected and three of them dated (Table 1). Although in a stratigraphically older position, samples CH-W01 and CH-W02 yielded ages younger (AD1680-1940 and AD1488-1950, respectively) than CH-W07 (AD1475-1660). This discrepancy may be due to the fact that sample CH-W07 is a small fragment of detrital charcoal included in higher energy deposits and thus may have experienced important reworking and transportation. Should this be the case, according to CH-W01, we can conclude that the sequence exposed in the trench is younger than 300 yr.

The **1999 earthquake** is recorded on various strands of the main and secondary fault zones, which either reach the surface, or deform the uppermost stratigraphic unit *a*, with or without discrete vertical displacements. A small scarplet with a free face, superimposed on the broader flexure, is still visible at fault zone A (Fig 7D).

Evidence for two paleoearthquakes predating 1999 was also found. Paleo-earthquake **CH-2** can be proposed based on upward fault terminations at the base or within the lower part of unit *d* and consequent smaller deformation of this unit with respect to the gravel units *e* and *g* together with the intervening silty sand layer (unit *f*). Because units *h* to *n* are intensely deformed by fault strands that terminate in, or below unit *g*, we set an older event horizon **CH-3** at the top of unit *j*. However, because the

southern splay of fault zone A terminates within unit *g*, this event horizon may be set also close to the top of *g*.

Based on the limited radiocarbon dating available, and assuming sample CH-W07 is reworked, the two paleoearthquakes recognized in the trench have taken place after approx. AD 1680 and before 1999.

2.4 The Cinarli trench (CIN)

The Cinarli trench is located in an area were repeated activity along the Düzce fault is testified by a series of tectonic ridges that have developed on Pleistocene and Holocene deposits of a bajada formed in front of the Almacik rangefront (figs. 1B and 8A). These ridges strongly control the drainage pattern and alluvial fan deposition, causing damming of streams and development of marsh areas. The trench was opened across a compound scarp along which one of the 1999 traces of surface faulting occurred with ca. 1 m vertical and 0.5 m dextral movements, producing the damming of a creek flowing toward the Düzce plain. A second rupture occurred a few meters to the south, almost parallel to the first but with only horizontal slip component (ca. 3m) (Akyuz et al., 2000 and 2002; Pucci et al., 2006a). The deposits exposed in the trench walls can be subdivided into two groups (see caption of fig. 8 for stratigraphy): those close to the compound normal scarp to the north, which are mainly fluvial channel and scarp-derived sediments, and those related to the stream flood plain to the south (*q2, r*, *s*, *t*), that are mainly silt, clay, and fine sand with important organic content. Deposition was clearly episodic and rootlet beds suggest some hiatuses. Two fault zones deform the entire sequence and coincide with the ruptures produced by the 1999 earthquake (figs. 8B and C and fig. 9). Fault zone A is very clear, shows an important vertical component and consists in a main trace splaying into several strands ca. 1.5 m below the surface.

The geometry of fault zone B was not documented in detail because instability caused continuous collapse of the walls at its location.

To provide a timeframe to the exposed sediments, we collected several samples for ^{14}C and ^{210}Pb analyses.

All the Radiocarbon-dated samples (Table 1 and fig. 8C) are charcoal and wood fragments; they thus provide maximum-limiting ages for the hosting layers. Reworking can explain the incongruous ages obtained from layer *s* (samples CIN1-500 and CIN1-W310) and the stratigraphic inversion between CIN-W16 and CIN-W03. Because of this, in the following interpretation we use only the younger ages. Layers *g*, *h*, *b* and *n* to *s* were all deposited during the past ca. 700 yr (AD1280, sample CIN1-W500), unit *q* and those above it are younger than AD1675, whereas, sample CIN-W03, likely derived from the erosion of the scarp, can be used to infer that the top layers of the gravel sequence north of the main fault zone are deposited ca. AD1270 or after.

^{210}Pb analysis was used to better constrain the age of the younger part of the stratigraphy. Sampling was performed in the southern part of the trench, from the surface to the top of the gravel unit *t* (fig. 9).

^{210}Pb activity shows a broadly exponential decline with depth. The ^{210}Pb-derived chronology extends from the surface to around 40cm depth (*i.e.*, units *n*, *p* and *q2* in fig. 8). Below this depth, activity levels were at a background level, probably reflecting in situ ^{210}Pb production, so the CRS model-generated dates that are unreliable. The mean accumulation rate over the last century has been approximately 0.4 cm a^{-1} since unit q2), with an increase in accumulation rates in the late 1990s (ca. 0.6 cm/yr.). Some caution is needed with such 'average' figures as deposition was clearly non-continuous. A decline in ^{210}Pb activity identified at 2cm depth (unit n), probably reflects the input of 'old'

material derived from a nearby eroding surface. The age-depth module places this event in the AD1990s.

The **1999 ruptures** were still clearly visible along the main fault zone. The ruptures occurring close to the bottom of the compound scarp showed four closely spaced splays that produced a clear vertical offset of the surface, with the southern side down. Conversely, evidence for 1999 surface faulting was less clear at fault zone B, where important shearing up to the uppermost clay units is suggested by the absence of clear contacts in the deformation zone and instability of the trench wall. The 1999 coseismic deformation caused damming of the stream and consequent flooding of the area. ^{210}Pb analysis shows evidence for inclusion of old sediments in the marsh that suppressed ^{210}Pb activity. This observation can be interpreted as the direct consequence of erosion of the newly formed scarp and intensification of human activities to clear the area.

Evidence for two paleoearthquakes predating the 1999 was found in this trench too (fig. 8C). The **penultimate event (CIN-2)** is recognized on the basis of the presence of a wedge-shaped unit of scarp-derived colluvium (unit *b*), interfingering with recent marsh deposits to the south (unit *m*). The colluvium rests on top of a unit of grey clay (unit *q*) and a brown-orange silt close to the scarp (unit *g*). One other possibility is that event CIN-2 produced a depression between the two fault zones and caused ponding and fast sedimentation of unit *q*, followed by the deposition of the colluvial wedge unit *b*. This hypothesis may be supported also by the presence of a paleosol below the grey clay of unit *q*, which suggests an abrupt change in depositional environment, from a stable ground surface to one similar to that related to the fresh water inundation following the 1999 event. In this case, the event horizon would be at the base of unit *q*.

Evidence for a **third earthquake** back in time **(CIN-3)** is found at fault zone B. Faulting during this event juxtaposed the yellow-brown gravel (unit *t*) and black sandy silt (unit *s*) against the grey clay (unit *i*). Coseismic damming of the local stream resulted in deposition of drift wood (top of unit *s*) and a change from an intermittent infill of an abandoned channel to a low-energy overbank and back-swamp depositional environment (unit *r* and above).

By merging results from both ^{14}C and ^{210}Pb analyses, we tried to constrain the timing of paleoearthquakes. Radiocarbon dating shows that unit *q*, which probably pre-date event CIN-2, is younger than AD1675 (CIN1-W16). Because this age derives from detrital charcoal, it provides a maximum age for the hosting sediments. Therefore, regardless of whether the event horizon is at the base or top of unit *q* (see discussion above), we assume the age of sample CIN1-W16 to be a maximum age for the CIN-2 earthquake. By correlating layers at both sides of fault zone B, ^{210}Pb suggests that unit q2 and those above it deposited during the past ca. 100 yr. If this is correct, the penultimate event CIN-2occurred at about the end of the 19th century.

According to sample CIN1-W500 that was collected at the top of the sediments faulted by event CIN-3, this is younger than AD1280. If we consider valid extrapolating the rates of sedimentation obtained from ^{210}Pb for the upper 40 cm to the CIN-3 event horizon, event CIN-3 may be as young as AD1700.

2.5 The Aksu trench

The Aksu site is located near the western termination of the November 1999 earthquake rupture (fig. 1). In this area the 1999 surface rupture zone generally runs at the base of the range front and has a predominantly vertical sense of displacement. Measured coseismic offsets were ca. 0.3 dextral and 0.7-1.7m vertical (Akyüz et al.,

2000 and 2002; Pucci et al., *submitted*). At the trench site the 1999 rupture strikes about E-W, cutting through a major alluvial fan and deposits of a younger fan developed on it. The rupture is composed by a main N-facing scarp and an antithetic almost parallel one, both showing evidence of cumulative slip (fig. 10). For logistic reasons the trench was dug across the antithetic scarp.

The trench was excavated in a NNE-SSW direction and (fig. 11) and exposed deposits that can be subdivided into three groups. The uppermost (units *a*-*c*) are soil horizons. The second group includes all the slope-wash and colluvial deposits (units *d* to *m*). The third group includes the alluvial fan layers (units *n* and *p*). A description of all stratigraphic units is given in figure 11. We found a single fault zone in the northern part of the trench, coincident with the 1999 antithetic scarp (figs. 11A and C), which separates the alluvial fan from the colluvial-slope wash units. The fault zone is formed by several sub-vertical splays which become more numerous at the trench bottom.

In order to constrain the age of the exposed sediments, we dated two charcoal samples. The radiocarbon age of a sample collected from the oldest of the colluvial/slope-wash units (sample AK-W06) indicates that the post-alluvial fan deposits are younger than AD890. Sample AK-W29, collected at the top of unit *g*, indicates that the upper meter of sediments is younger than 300 yr.

A broken piece of glass found ca. 80 cm below the surface within unit *e* (figs.11A and D) is clearly transported material, and thus it provides a maximum age for the enclosing deposit. Based on its thickness, weight, colour, type of fracture, inclusions, wall regularity etc, an age of AD1880-1950 is suggested (A. Delfino, pers. communication).

The **1999** earthquake ruptures still appear in the trench location as a 30 cm-high free face. The same amount of offset can be measured at least at the base of soil *b* (fig.

11A). On the basis of stratigraphic and structural relations, and taking into consideration the fact that this trench was excavated across a secondary antithetic splay of the 1999 main ruptures, which may not necessarily record all the surface faulting earthquakes that have occurred at this location, we found evidence for a minimum of two paleoearthquakes predating 1999 (fig. 11A). The penultimate event (**AKSU-2**) is well defined by the distinct upward termination of several fault splays and important downward increase of deformation below unit *e*. Unit *f* at the southern end of the trench is a wedge-shaped deposit, formed by coarse gravel different from that of the units above and below it. This unit is interpreted as the northern tip of a scarp-derived colluvium related to the post-event erosion of the main scarp immediately south of the trench. This strengthens the location of an event horizon at the contact between *e* and *g*.

At least one previous paleo-event (**AKSU-3**) is responsible for the intense shearing of the alluvial fan deposits (unit *p*, completely missing in the hangingwall of the antithetic fault zone), and of the subsequent deposition of the colluvial unit *i*. This latter unit is likely to have been deposited in a coseismic depression formed between the main and antithetic faults. The event horizon of AKSU-3 can be tentatively placed at the top of the alluvial fan deposits (unit *p*).

With the available ages, we can constrain the age of the penultimate earthquake (AKSU-2) sometime after the deposition of unit *g* and before the age of the glass, that is, after AD1670 (AK-W29) and before AD1880-1950 (AK-GLASS). Because the event horizon is substantially closer to the glass sample we suggest that AKSU-2 occurred close to the younger part of this interval. If unit *i* represents a post-event deposit following the occurrence of AKSU-3 and the age of sample AK-W06 is not substantially older than the hosting unit, this paleo-earthquake should have occurred just before or close in time to AD890-1020. This is because being the dated sample a small

piece of charcoal enclosed in a scarp-derived deposit, it probably comes from the erosion of the top of the scarp; thus, it may represent the age of the ground surface at the time of the event and not necessarily the age of the colluvium post-dating the event.

3. The paleoearthquakes of the Düzce fault

On the basis of sedimentary and structural relations, we found in all the trenches evidence for 2 to 3 surface faulting paleoearthquakes pre-dating the 1999 event.

Radiocarbon dating was rather problematic due to sample characteristics and their young ages, resulting in possible age ranges of occurrence of paleoearthquakes that are quite broad. Still, by using ^{210}Pb analyses and archaeological information with all the already discussed limitations, and by merging the radiocarbon results obtained from all the trenches it is possible to propose a seismic history for the Düzce fault for the past 1000-1200 yr.

Under the assumption that, similarly to the 1999 event, paleoearthquakes on the Düzce fault ruptured the whole fault, we correlate events between different trenches on the basis of their age compatibility and local sequence of the events. This assumption is considered likely because, as discussed in the initial part of this paper, the 40-km long Düzce fault appears to be controlled by two strong and persistent boundaries: the junction to the Karadere fault to the west, and the Bakacak-Elmalik releasing step over to the east.

Table 2 and figure 12 show the age ranges of the paleoearthquakes recognized in each trench and their correlation. We named the correlated paleoearthquakes of the Düzce fault prior to 1999 event as DUZ2, DUZ3 etc. Evidence for each of them is derived from different trenches. As already said, evidence for the 1999 surface ruptures

are clear in all the trenches. On the contrary, evidence for the other Düzce events is not found in every trench. Among the reasons for this missing information we can consider: successive event overprint (the same fault trace is activated with horizontal movement during younger faulting events), erosion of sediments containing the event horizon, exposure of secondary structures only, difficulty in the recognition due to deformation being too complex in unfavourable sediments (lacking bedding), etc. Event DUZ2 was found in all the trenches with exception for Men5 and Kay. For this latter one, uncertainty exists with the correlation of event Kay2 with DUZ2 or DUZ3. Event DUZ3 was found in all the trenches with exception of AKSU site and possibly Kay (see DUZ2 for this latter). Evidence for both DUZ4 and DUZ5 was found only at Kaynasli with support from Men5 and AKSU, respectively.

Merging radiocarbon ages from different trenches to constrain the age of DUZ2 yields the occurrence of this event sometime in the past 300 yr. According to historical documentation, we can assume that no events on this fault occurred during the 20th century. Thus, DUZ2 occurred between AD1700 and 1900. ^{210}Pb analysis from Cinarli trench (figs. 8 and 9) and the age estimate of the piece of glass from Aksu trench (figs. 11A and D) constrain the age of DUZ2 near AD1900. As already mentioned, local people living near the Mengencik (Men) site reported to us a surface faulting earthquake at the end of the 19th century. Unfortunately, no independent evidence for this has been found yet. However, because this information fits well with the results from trenching, we take this information as a possible reference.

On the basis of radiocarbon dating, the occurrence of DUZ3 is confined to the same age interval as DUZ2, *i.e.*, during the past 300 yr. For the reasons exposed above and because this event is stratigraphically older than DUZ2 we can exclude this has

occurred after AD1900. Also in this case, ^{210}Pb analysis can be used to constrain further the age of this event to the older part of the interval, *i.e*., near AD1700.

Finally, limited age constraints exist for DUZ4 and DUZ5 that, from radiocarbon dating, are expected to have occurred between AD1185-1640 and AD685-1220, respectively. On the basis of stratigraphic considerations from AKSU trench (see above), the age of occurrence of DUZ5 can be limited in the range AD800-1000.

4. Discussion

4.1 Comparison of paleoearthquakes with historical record

On the basis of paleoseismological investigation we found evidence for four surface faulting paleoearthquakes that ruptured the Düzce fault before the November, 1999 event. The two most recent ones occurred during the past 300 yr, possibly around AD1900 and 1700. The two older occurred at AD1185-1640 and AD800-1000 (figs. 12 and 13). No obvious correlation of the paleoearthquakes with the large events reported in the historical catalogues (Ambraseys and Finkel, 1995; Guidoboni et al. 1994; Guidoboni and Comastri, 2005) can be proposed. In fact, as already mentioned, even though historical information for damaging earthquakes exists in Turkey for the past 2000 yr, we found no clear information connecting specific earthquakes to the Duzce fault. This is probably a consequence of the limited settlement of the Düzce area that, also nowadays is mainly an agricultural centre. The only historical earthquakes that are known to have produced damage near the Düzce fault are the (a) AD1719 earthquake, that possibly ruptured the whole Izmit and Karadere faults (b) AD1754 located in the Sapanca area, (c) AD1878 earthquake, possibly located on the Hendek fault or in the Akyazi plain, (d) AD1894, which occurred on the Izmit fault segment and (e) AD967

felt in the area of Bolu (Ambraseys and Finkel, 1995; Ambraseys, 2002; Atakan, 2002; King et al., 2001 - see fig. 1 for earthquake mezoseismal areas).

It is interesting to notice that, according to our paleoseismological results, the AD1719, AD1878, AD1894 and AD967 are compatible with a rupture of the Düzce fault. This may suggest a mislocation of some of these historical earthquakes that occurred on the Düzce fault and not on other structures or, alternatively, the occurrence of a cascade of events that ruptured, within a short interval of time, the Düzce and nearby faults (as in the case of the Izmit and Düzce 1999 earthquakes).

4.2. Comparison with results of previous paleoseismological studies on the Düzce fault

Previous paleoseismological investigations (Sugai et al., 2001; Emre et al., 2001, 2003a and 2003b; Hitchcock et al., 2003; Komut, 2005) show evidence for surface faulting paleoearthquakes during the past 2000 yr or more. In general, because of the location and type of depositional environment at trench sites, these works present a longer seismic history but lower detail. Our study focused instead on deposits going only a few centuries back (400-500 yrs). Figure 13 summarizes results from all previous works on the Düzce fault, together with those from the present work. In this synthesis, in order to make the dataset homogeneous, we re-interpreted age ranges for some of the previously published events, we excluded events with only one age constraint (es. Hitchcock et al. 2003, and Komut, 2005) and included only the events in the past two millennia.

In this work we have clear and independent stratigraphic evidence for the occurrence of three events, including 1999, during the past 300 yr (1999, DUZ2, DUZ3). On the contrary, the previous works show evidence for only one event

predating 1999 during the past 300-400 yr. As discussed above, the lack of evidence for one further event in the past 300 yr in previous works can be seen as a consequence of low resolution stratigraphy and structures (*i.e.*, evidence has been overprinted by the most recent event(s), low rates of deposition not allowing to recognize upper terminations of faults, etc.). A noteworthy case for this is trench Men5 that, although located only 25 m apart from Men1, besides the 1999 event, shows evidence for only one surface faulting paleo-earthquake in the same package of sediments where in Men1 there is evidence for two. The previous event (DUZ4) is found only in the present work at ca AD 1200-1650, whereas the oldest (DUZ5) may correlate with an event at ca AD1000 found by Sugai et al. (2001) and Emre et al. (2001, 2003a and 2003b). Two older events at ca. AD 600 and ca. AD200 are found by Sugai et al. (2001) (fig 13).

4.3. Implications for earthquake recurrence

On the basis of the results from this work, five events since AD685-1220 (possibly AD800-1000) yield an average recurrence for the Düzce fault in the range of 200-325 yr (possibly 250-300yr). However, the three most recent events, including 1999, appear more closely spaced. Longer average recurrence intervals are further suggested if we include paleoearthquakes from previous studies, which reach farther back in time (the last 2000 yrs). The synthetic dataset in fig. 13 indicates average recurrence intervals of ca. 400 yr for the four older events, and ca. 200 yr for the four last earthquakes. For comparison, using all seven paleo-earthquakes events, we obtain an average recurrence interval of about 320 yr.

We have to note, that less frequent earthquakes as we move back in time may merely be the result of lack of complete sedimentary sequences for paleoseismological interpretation. Should we consider the paleoseismic record to be complete, the sequence

depicted in fig. 13 would be suggestive of earthquake clustering in time (Wallace, 1987).

If such a change in earthquake frequency is after all true, it would indicate an important change in the strain release and partitioning in this sector of the NAFZ or an increased interaction between the Düzce and Izmit faults (as in 1999). In fact, even though with uncertainties, the seismic history of the Izmit fault during the past 400yr (both from historical and paleoseismological evidence - Ambraseys and Finkel, 1995; Ambraseys, 2002; Kingler et al., 2000; Rockwell et al., 2001; Rockwell and Meghraoui, 2003; AA.VV., 2005) indicates events occurring close in time to at least the past three earthquakes of the Düzce fault (1999, DUZ2 and DUZ3). Thus, the 1999 earthquake sequence would be the typical behavior of this sector of the NAFZ faults.

4.4. Insights on the slip rate of the Duzce fault

As already mentioned, no measurements of coseismic offset from trenches were possible. If we assume that the Duzce fault is a segment of the NAFZ defined by persistent segment boundaries (see introduction) and that the 1999 earthquake is characteristic for this fault (*sensu* Schwartz & Coppersmith, 1984), we may use the average recurrence time from our study and the 2.7 m average of coseismic slip observed in 1999 to obtain a first approximation of fault slip rate.

If we take the more conservative average recurrence time, calculated including all the seven events occurred during the past ca. two millennia (i.e., 320 yr), and an average coseismic slip of 2.7 m, we obtain a slip rate of ca. 8.4 mm/yr, which may be as low as 6.7 and as high as 13.5 mm/yr if we use the two extreme recurrence distributions (400 and 200yr, respectively). The highest part of this range is compatible with a geological slip rate of 14+-2 mm/yr for the past 60kyr based on offset fluvial terraces in

the central part of the fault (Pucci et al., submitted) and the ca. 10 mm/yr estimate from GPS measuments (Ayhan et al., 2001). This suggest that the ca. 2 cm/yr of motion accommodated by the NAFZ in this area appears almost equally partitioned between the Duzce and Mudurnu faults.

5. Conclusions

Trenching along the Duzce fault has provided new data about the earthquake history of this part of the NAFZ as well as new insights on earthquake recurrence.

Although with uncertainties in dating, we recognized geological evidence of four surface faulting earthquakes prior to 1999. These are dated on the basis of radiocarbon, 210Pb and archaeological information and can be summarized as follows:

DUZ2: AD1685-1900, possibly end of 19th century;

DUZ3 : AD1685-1900, possibly close to AD1700;

DUZ4: AD1185-1640

DUZ5: possibly AD800-1000

From the historical catalogues, none of these earthquakes is known to have ruptured the Duzce fault. However, the fact that some of these paleoearthquakes can be correlated to historical earthquakes attributed to nearby faults, allows for the possibility that these earthquakes (AD967, 1719, 1878 and 1894) may have been accompanied by ruptures also at the Duzce fault, in cascades of earthquakes similar to the Izmit-Duzce cascade of 1999.

Our paleoseismological results, merged with those from previous papers for the past two millennia, are suggestive of a bimodal recurrence distribution (ca. 400 and 200

yrs) yielding an overall average recurrence of 320 yr. Under the assumption that the Duzce fault generates characteristic earthquakes, these average recurrence intervals, allow for first approximation slip rate estimates of 8.4 mm/yr, within a range of 13.5 and 6.7 mm/yr, respectively.

Acknowledgments. This work was supported by EC project RELIEF (EVG1-CT-2002-00069) and benefited of the field support and throughout discussion of M. Meghraoui, S. Akyuz, G. Uçarçus, A. Dikbas, D. Satir and G. Sunal. We also wish to thank local authorities and land owners for letting us excavate trenches.

References

AA.VV., (2005), EC Relief project "Large Earthquake Faulting and Implications for the Seismic Hazard Assessment in Europe: The Izmit-Duzce earthquake sequence of August-November 1999 (Turkey, Mw 7.4, 7.1)", EVG1-CT-2002-00069, final report, www.ingv.it/paleo/RELIEF.

Akyüz, H.S., A.A. Barka, E. Altunel, R.D. Hartleb, and G. Sunal (2000), Field observations and slip distribution of the November 12, 1999 Düzce earthquake (M=7.1), Bolu - Turkey. In: A.A. Barka et al. (Eds.), The 1999 Izmit and Düzce earthquakes; preliminary results. Istanbul Technical University, Istanbul, Turkey, pp. 63-70.

Akyüz, H.S., R.D. Hartleb, A.A. Barka, E. Altunel, G. Sunal, B. Meyer and R. Armijo, (2002), Surface rupture and slip distribution of the 12 November 1999 Düzce

earthquake (M7.1), North Anatolian Fault, Bolu, Turkey. Bulletin of the Seismological Society of America 92 (1), 61-66.

Altunel, E., A.A. Barka, Z. Çakır, Ö. Kozacı, C. Hitchcock, J. Helms, J. Bachhuber and W. Lettis (2000), What goes on at the eastern termination of the November 12, 1999 Düzce earthquake, M=7.2, North Anatolian Fault, Turkey. American Geophysical Fall Meeting, California, USA, Abstracts, p. F816.

Ambraseys N.N (2002), The seismic activity of the Marmara Sea region over the last 2000 years, *Bulletin of the Seismological Society of America*, *92* (1), 1-18.

Ambraseys N.N. and C.F. Finkel (1995), The seismicity of Turkey and adjacent areas: a historical review, 1500-1800, *Muhittin Salih Eren*, 240 pp., Istanbul.

Appleby P.G. (2001), Chronostratigraphic techniques in recent sediments. IN Last, W.M., and Smol, J.P. (eds) Tracking environmental Changes Using Lake Sediments. Volume 1: Basin Analysis, Coring and Chronological Techniques. Kluwer, Dordrecht, The Netherlands. Pp171-203

Armijo R., B. Meyer, A. Hubert and A.A. Barka (1999), Westward propagation of the North Anatolian fault into the northern Aegean: Timing and kinematics. Geology 27 (3), 267-270.

Ayhan, M.A., C. Demir, A. Kiliçoglu, I. Sanli, and S.M. Nakiboglu (1999), Crustal motion around the western segment of the north Anatolian fault zone: geodetic

measurements and geophysical interpretation, International Union of Geodesy and Geophysics (IUGG99), Birmingham, United Kingdom, 18-30 July.

Ayhan, M.E., R. Burgmann, S. McClusky, O. Lenk, B. Aktug, E. Herece and R.E. Reilinger (2001), Kinematics of the Mw=7.2, 12 November 1999, Düzce, Turkey earthquake, *Geophys. Res. Let.*, 28 (2), 367-370.

Atakan K., A. Ojeda, M. Meghraoui, A. A. Barka, M. Erdik, and A. Bodare (2002), Seismic Hazard in Istanbul following the 17 August 1999 Iÿzmit and 12 November 1999 Duzce Earthquakes, *Bull. Seism. Soc. Am.*, 92, 1, 466-482.

Barka, A.A. (1981), Seismo-tectonic aspects of the North Anatolian fault zone, Ph.D. thesis, 335 pp., Univ. of Bristol, England.

Barka, A.A. (1992), The North Anatolian fault zone. Annales Tectonicae 6, 164-195.

Barka A.A. and K. Kadinski-Cade (1988), Strike-slip fault geometry in Turkey and its influence on earthquake activity. Tectonophysics 7, 663-684.

Barka, A.A., and P.L. Hancock (1984), Neotectonic deformation patterns in the convex-northwards arc of the North Anatolian fault zone, *J. Geol. Soc. London,* Spec. Pub., 17, 763-774.

Barka, A.A, and M. Erdik (1993), Site specific fault rupture hazard investigation for the viaduct n°1 and 1A of the Gümüşova-Gerede motorway. Unpublished report.

Barka, A.A., E. Altunel, S. Akyüz, Z. Çakır, Ö. Kozacı, W. Lettis, J. Bachhuber, C. Hitchcock and J. Helms (2001), Seismic Activity and Fault Segmentation of the NAF in the Bolu Mountain: Relationship between the November 12, 1999 and the February 1, 1944 Earthquakes. EUG XI Meeting, Abstracts, Strasbourg, France, p. 295.

Bradley, R.S. (1985), Quaternary Paleoclimatology – Methods pf Paeoclimatic Reconstruction. Unwin Hyman, London.

Christie-Blick, N. and K.T. Biddle (1985), Deformation and basin formation along strike-slip faults, in *Strike-slip Deformation, Basin Formation and Sedimentation*, K.T. Biddle and N. Christie-Blick (Editors), Soc.Econ. Paleont. Min. Spec. Publ.,1-34.

Cundy A.B. and Stewart. I.S. (2004), Dating recent colluvial sequences with Pb-210 and Cs-137 along an active fault scarp, the Eliki Fault, Gulf of Corinth, Greece. Tectonophysics 386, 147-156.

Emre, Ö., T.Y. Duman, S. Toda, M. Okuno, A. Dogan, S. Ozalp, H. Tsutsumi, F. Tokay, T. Haraguchi, H. Kondo, N. Subito and T. Nakamura (2001), Paleoseismologic Findings on the Düzce Fault: North Anatolian Fault Zone, NW Turkey. American Geophysical Union, Fall Meeting 2001, abstract

Emre, Ö., Y. Awata and T. Duman (Eds.) (2003a), Surface rupture associated with the 17 August 1999 Izmit earthquake. General Directorate of Mineral Research and Exploration, Ankara, Turkey, ISBN: 975-6595-53-1, pp. 29–271.

Emre, Ö., S. Toda, T.Y. Duman, T. Sugai, A. Dogan, Y. Awata, M.Okuno, H. Tsutsumi, S. Ozalp and F. Tokay (2003b), Recurrence of the large earthquakes on the 1999 Izmit and Düzce surface ruptures, North Anatolian Fault, Turkey. EGS-AGU-EUG Joint Assembly, Abstracts, 6-11 April 2003, Nice, France.

Giudoboni, E., A. Comastri and G. Traina (1994), Catalogue of ancient earthquakes in the Mediterranean area up to the 10th century. S.G.A., Storia Geofisica Ambiente and I.N.G., Istituto Nazionale di Geofisica (eds.), Bologna, pp 504.

Guidoboni E., and A. Comastri (2005), Catalogue of earthquakes and tsunamis in the Mediterranean area from the 11/th to the 15/th century. S.G.A., Storia Geofisica Ambiente (ed.), Bologna, pp 1037.

Hitchcock, C., E. Altunel, A.A Barka, J. Bachhber, W. Lettis, Ö. Kozci, J. Helms and S. Lindvall (2003), Timing of Late Holocene earthquakes on the eastern Düzce fault and implications for slip transfer between the southern and the northern strands of the North Anatolian Fault System, Bolu, Turkey. Turkish J. Earth Sci., 12 (1), 119-136.

Hubert-Ferrari, A., R. Armijo, G. King, B. Meyer and A. Barka (2002), Morphology, displacement, and slip rates along the northern Anatolian Fault, Turkey. J. Geophys. Res. 107 (B10), 2235, doi: 10.1029/2001JB000393.

Kahle H. G., M. Cocard, Y. Peter, A. Geiger, R. Reilinger, S.C. McClusky, R. King, A. Barka and G. Veis (1999), GPS-derived strain rate field within the boundary zones of the Eurasian, African, and Arabian Plates. J. Geophy. Res. 105 (B3), 23 353-23 370.

Kahle H. G., M. Cocard, Y. Peter, A. Geiger, R. Reilinger, A. Barka and G. Veis (2000), GPS-derived strain rate field within the boundary zones of the Eurasian, African, and Arabian Plates. J. Geophy. Res. 105 (B3), 23 353-23 370.

King,.G., A. Hubert-Ferrari, S.S. Nalbant, B. Meyer, R. Armijo, D. Bowman (2001), Coulomb interactions and the 17 August 1999 Izmit, Turkey earthquake, Earth and Planetary Sciences, Tectonique / Tectonics 333, 557-569.

Klinger, Y., T. Dawson, A.Akoglu, T. Gonzalez, A. Meltzner, K. Sieh, K., T. Rockwell, A. Barka, R. Langridge, D. Ragona, and E. Altunel (2000), Paleoseismic Evidences for Prior Ruptures Similar to the August 1999 Event on the North Anatolian Fault, Eos Trans. AGU, 81 (48), Fall Meet. Suppl., 2000.

Komut T. (2005), Paleoseismological studies on Düzce fault and geological data on the seismogenic sources in the vicinity of Düzce area, Kandilli Observatory and Earthquake Research Institute Boğaziçi University, Ph.D. Thesis, pp. 155.

Lettis, W., J. Bachhuber, R. Witter, C. Brankman, C.E. Randolph, A. Barka, W.D. Page and A. Kaya (2002), Influence of releasing step-overs on surface fault rupture and fault segmentation: examples from the 17 August 1999 Izmit earthquake on the North Anatolian Fault, Turkey, *Seism. Soc. Am. Bull.*, *92* (1), 19-42.

McClusky, S.C., A. Balassanian, A.A. Barka, C. Demir and S. Ergintav (2000), Global positioning system constrain on plate kinematics and dynamics in the eastern Medditerranean and Caucasus. J. Geophy. Res. 105 (B3), 5695-5720.

McKenzie, D.P. (1972), Active tectonics of the Mediterranean region. Geophys. J. R. Astron. Soc. 30, 109-185.

Okay, A.l., E. Demirbag, H. Kurt, N. Okay, I. Kuscu (1999), An active, deep marine strike-slip basin along the North Anatolian Fault in Turkey. Tectonics 18 (1), 129-147

Pucci, S., Palyvos, N., Zabci, C., Pantosti, D., and M. Barchi (2006a), Coseismic ruptures and tectonic landforms along the Düzce segment of the North Anatolian Fault Zone (Ms 7.1, Nov. 1999). J. Geophys. Res., 111, B06312, doi: 10.1029/2004JB003578.

Pucci S., D. Pantosti, M. Barchi and N. Palyvos (2006b), Evolution and complexity of the seismogenic Düzce fault zone (Turkey) depicted by coseismic ruptures, Plio-Quaternary structural pattern and geomorphology. Earth Planet. Sci. Lett., submitted.

Reilinger, R.E., S.C. McClusky, M.B. Oral, W. King and M.N. Toksöz (1997), Global Positioning, System measurements of present-day crustal movements in the Arabian-Africa-Eurasia plate collision zone. J. Geophy. Res. 102 (B5), 9983-9999.

Reilinger, R.E., Toksöz, M.N., McClusky and A.A. Barka (2000), 1999 Izmit, Turkey Earthquake was no surprise. GSA Today 10, 1-6.

Reimer, P.J., M.G.L. Baillie, E. Bard, A. Bayliss, J.W. Beck, C. Bertrand, P.G. Blackwell, C.E. Buck, G. Burr, K.B. Cutler, P.E. Damon, R.L. Edwards, R.G. Fairbanks, M. Friedrich, T.P. Guilderson, K.A. Hughen, B. Kromer, F.G. McCormac, S. Manning, C. Bronk Ramsey, R.W. Reimer, S. Remmele, J.R. Southon, M. Stuiver, S. Talamo, F.W. Taylor, J van der Plicht and C.E. Weyhenmeyer (2004), IntCal04 terrestrial radiocarbon age calibration, 0-26 cal kyr BP. Radiocarbon 46, 1029-1058.

Rockwell, T.K., B. Akbalik, A. Akoglu, E. Aksoy, A. Barka, D.Dier, M.Ferry, Y. Klinger, R.Langridge, M. Meghraoui, A.Meltzner, D. Ragona, D. Satir, G.Seitz, and G.Ucarkus (2001), Results of paleoseismic studies after the 1999 Izmit earthquake: Implications for seismic hazard to Istanbul: European Union of Geosciences meeting, 2001, Strasbourg, Abstracts, v. 1, p. 292.

Rockwell, T., and M. Meghraoui (2003), Paleoseismology near the Sea of Marmara: Implications on the constancy of segment boundaries and multi-segment ruptures, EGS - AGU - EUG Joint Assembly, Nice, France, Abstract #12947.

Sengör, A.M.C. (1979), The North Anatolian transform fault: Its age, offset and tectonic significance. J. Geol. Soc. London 136, 269-282.

Seymen, I. (1975), Tectonic characteristics of the North Anatolian fault zone in the Kelkit valley, Ph.D. thesis, Istanbul Technical Univ., Istanbul, Turkey, 192 pp.

Schwartz, D. P. and K. J. Coppersmith (1984), Fault behaviour and characteristic earthquakes: examples from the Wasatch and San Andreas fault zones, *J. Geophys. Res.*, 89, 5681-5698.

Straub, C., H. G. Kahle, and C. Schindler (1997), GPS and geologic estimates of the tectonic activity in the Marmara Sea region, NW Anatolia. J. Geophys. Res. 102 (B12), 27 587-27 601.

Stuiver, M., and Quay, P.D. (1980), Changes in atmospheric carbon-14 attributed to a variable sun. Science, 207, 11-19.

Stuiver, M., and P.J. Reimer (2005), Extended (super 14) C data base and revised CALIB 3.0 (super 14) C age calibration program. Radiocarbon 35, 215-230. 2005 CALIB 5.02

Sugai, T., Y. Awata, S. Toda, Ö. Emre, A. Dogan, S. Ozalp, T. Haraguchi, H. Kinoshita, K. Takada and M. Yamaguchi (2001), Paleoseismic investigation of the 1999 Düzce earthquake fault at Lake Efteni, North Anatolian fault system, Turkey. Annual Report on Active Fault and Paleoearthquake Researches No. 1, Active Fault Research Center, Japan.

Tokay, M. (1973), Geological observation on the North Anatolian fault zone between Gerede and Ilgaz, Proceedings of Symposium on the North Anatolian Fault Zone and Earthquake Belt, pp. 12–29, Mineral Research and Exploration Institute of Turkey, Ankara.

Wallace R.E. (1987), Grouping and migration of surface faulting and variation in slip rates on faults in the Great Basin province, Bull. Soc. Am., 77, 868-877.

Westaway, R. (1994), Present-day kinematics of the Middle-East and Eastern Mediterranean. J. Geophys. Res. 99, 12 071-12 090.

Wong, H K, T. Luedmann, A. Ulug and N. Gorur (1995), The Sea of Marmara; a plate boundary sea in an escape tectonic regime. Tectonophysics 244 (4), 231-250.

Figure captions

Figure 1 (A) Simplified trace of the North Anatolian Fault Zone west of the of the Bolu basin (see lower right inset for location of the area). Portions of the fault zone that ruptured during the 1999, earthquakes are shown. The mezoseismal areas of the historical earthquakes occurred near the Düzce fault segment are shown too (from Ambraseys and Finkel, 1995; Ambraseys, 2002; Atakan, 2002; King et al., 2001) **(B)** Trace of the 1999 surface ruptures along the Düzce fault (see dashed rectangle in figure 1A for location) and location of the five trench sites discussed in this paper (rectangles; KAY: Kaynasli; MEN: Mengencik; CH: Cakir Haci Ibrahim; CIN: Cinarli; AK: Aksu). Numbered hexagons are locations where trenching from other authors was performed (1. Hitchcock et al., 2003; 2. Tolga, 2005; 3. Emre et al. 2001, 2003a and 2003b; 4. Sugai et al., 2001).

Figure 2 (A) Simplified log of the main fault zones of the Kaynasli trench (KAY in fig 1B). Stars indicate event horizons, triangles are dated charcoal samples (details in Table 1). Stratigraphy: **a.** active brown silty soil; **b.** brown clayey-silty soil with clay patches (post 1999 earthquake deposit); **z.** clay and sand from underlying layers, injected in 1999 along the fault plane?; **c.** granular, brown silty soil, organic-rich with sparse pebbles with injected sand and clay from unit e at the base in the northern end of the trench; **d.** dark brown clayey-silty soil with injection of sand and clay from unit e; **k.** big stones in silty clay matrix with layers (2 to 4 cm thick) of silt, clay and sand at the bottom (interpreted as man made feature postdating event Kay2); **e.** laminated fine sand with important oxidation, sand, and fine to medium gravel in silty matrix; **f.** laminated dark grey fine sand and fine gravel in clayey-silty matrix, lenses of clay, oxidation; **g**.

light grey clay with sparse pebbles, penetration of roots; **h.** grey clay, fine to medium gravel in clay matrix, coarse pebbly layer at the base, roots penetration; **i.** medium to coarse pebbles in orange oxidized clay matrix; **m.** laminated coarse sand to coarse gravel with some silty matrix. Bluish dashed zones refers to coloration due to reduction. **(B)** View of the west wall of the trench. **(C)** Detail of fault zone 1 west wall. **(D)** Detail of fault zone 1 east wall.

Figure 3. (A) Detailed topographic map obtained by a 5000 DGPS survey of the Mengencik site (MEN site in fig 1B). The trace of the 1999 ruptures is still very clear (thick red line); trenches and main natural and artificial features are shown, green lines outline tectonic ridges; **(B)** aerial view of the site.

Figure 4. (A) Simplified log of the main fault zones of the Men1 trench (location in fig. 3). Stars indicate event horizons, black triangles are radiocarbon dated samples (details in Table 1), black rectangles are locations of samples for ^{210}Pb analysis, empty vertical rectangle encloses the deposits whose expected ^{210}Pb age is indicated above. Stratigraphy: **a.** root mat; **b.** yellow silt and fine sand intercalated to root mat layers; **c.** grey silt, organic with small concretions; **d.** yellow silt and clay with small nodules and sparse pebbles up to 1 cm, sand pockets at places **e.** grey silt, organic with small concretions (paleosol?); **f** grey silt, with a charcoal-rich layer at the bottom (fire?); **g.** yellow silt and clay, with mottles and concretions up to 3-4 cm.; **h.** sparse white marls fragments (mean size 1-2 cm) in brown-yellow silt; **i.** massive yellow-brown silt and clay, orange mottles, 1-2 cm iron nodules, few sparse large clasts from the marls, pieces of ceramics; **k.** brownish silt, blocky, organic, paleosol locally interbedded with yellow silt; **m.** pale yellow silt, blocky and dry; **n.** massive yellow-brown silt, with iron nodules

and locally gravel channels (gr) more clay rich at the bottom. **(B)** View of trench from south, 1999 surface ruptures are shown by arrows; **(C**) View of the main zone of faulting, west wall; **(D)** Summary of results for 210Pb dating.

Figure 5. (A) View of the west wall of trench Men5 (location in fig. 3), notice the main fault zone that here appears as a negative flower structure; **(B)** Simplified log of the main fault zone of the Men5 trench west wall. Stars indicate event horizons, black triangles are sample locations (details in Table 1). Stratigraphy: **a.** root mat; **b.** yellow silt and fine sand frequently containing root mat layers; **c.** organic grey silt, with small concretions; **d.** yellow silt and clay with small nodules and sparse pebbles up to 1 cm, sand pockets at places; **ee.** organic grey silt, with small concretions, with a charcoal rich layer at the bottom (fire?), possibly deposited in a scarp-controlled pond; **gg.** white silt with sparse fragments of marls up to 3 cm size; **j.** yellow silty clay, with local concentration of fine granular gravel; **y.** yellow-brown clay mottled and with oxidised small clasts; **w.** mottled brown organic clay; **z.** brown-reddish organic clay and silt; **aa.** organic brownish silt, blocky, locally interlayered with yellow silt; **p.** blocky yellow silt; **q.** sheared yellow-grey silt with rare nodules; **r.** highly compact pale yellow silt with sparse clasts of marls and ceramics; **s;** yellowish silty clay particularly sheared in the fault zone.

Figure 6. (A) View from north of the Men6 trench (location in fig. 3), arrows point to the main 1999 surface ruptures; **(B)** Simplified log of the southern fault zone west wall; **(C)** view of the southern fault zone east wall; **(D)** Simplified log of the southern fault zone east wall. Stratigraphy in panels B and D: **a.** active soil, generally ploughed up to 30 cm depth; **b.** organic silt; **c.** yellow silt; **d.** organic silt; **e.** massive

yellow silt with small sandy and granular channels at the base; **f.** burn layer and reworked material from the burn layer near fault C; **g.** yellow silt and fine sand with laminations of white clay and sand, locally convoluted; **h.** yellowish silt, it is possibly equivalent to units b-g and include q; **i.** organic pale grey silty-sand, layered; **k.** organic grey silty-sand with sparse pebbles and small charcoal; **m.** red silt, with granules, intense weathering; **n.** grey silt, locally more clay rich; **p.** dark yellow silt, drier than the lower one; **q.** orange (weathered) silt with a whitish package at the base; **r.** massive yellow silt and silty sand (probably derived from the compaction of different layers) including also roots and organic-rich beds; **s.** massive clayey silt to fine sand; same origin as r; **t.** blocky silt, light brown with a orange layer in the middle possibly correlated with b; **u.** dark yellow silt with weathered iron nodules; **z.** fine gravel in a silty-sandy matrix, gutter channels. Stars indicate event horizons, black triangles are sample locations (details in Table 1).

Figure 7. (A) Geomorphological map of the Caki Haci Ibrahim trench area; contours every 10 m from 1:25,000 topographic maps. **(B)** Microtopographic map of the trenched scarp from a 860 point total station survey. Notice the small left-stepping scarps; green rectangle outlines the trench, blue, dashed line is an ephimeral drainage. **(C)** View of the 1999 scarp looking north, dashed lines underline top and base of the scarp, trench in the left background. **(D)** Mosaic of the main fault zone with simplified line-drawing and shading from the field trench log. Stars indicate event horizons, black triangles are sample locations (details in Table 1); the * next to the sample name indicate that the sample was located outside of this panel and its position is thus based on stratigraphic correlation. Stratigraphy: **a.** coarse sand fining upwards to sandy silt or silt, locally fine pebbles at the bottom; organic soil developed on the upper part; **b.** very

coarse pebbles, cobbles and small boulders in matrix of fine pebbles and coarse sand; **d.** coarse sands interfingering with pebbles (up to coarse)**; e.** medium to coarse pebbles, small and large cobbles in matrix of fine pebbles and coarse sand; **f.** silty sand and very fine pebbles. Includes sparse very coarse pebbles; **g.** very coarse pebbles, cobbles and small boulders in granular loose matrix; **h.** silt and sand; **i.** alternating beds of coarse sands, fine pebbles and silt; **j.** silt and silty sand; **k.** silt, sand, fine pebbles and sparse coarse pebble; **m.** grey clay including large pieces of wood, with coarse sand and fine pebbles on top; **n.** silt including layers of sand and fine pebbles.

Figure 8. (A) Geomorphological map of the Cinarli trench area (location in fig. 1B). **(B)** View of the normal fault zone A (see panel C) **(C)** Simplified log of the west wall. Stars indicate event horizons; black triangles are sample locations (details in Table 1); vertical rectangle shows the sequence sampled for ^{210}Pb, the filled upper portion is the part for which the age-depth model of fig 9C is considered reliable. Stratigraphy: **a.** active soil; **b.** colluvium, silty fine sand with sparse round pebbles, finer southward, interpreted as scarp-derived deposit post-dating the pre-1999 event; **b2.** silty fine sand with few rounded pebbles; **c.** gravel in pale orange silty sand matrix, with big (6-8 cm) rounded pebbles; **d.** channel deposits, with big rounded pebbles in a orange-brown matrix; **e.** channel deposits, with few small rounded pebbles in a brownish matrix; **f.** same as e but with a\grey-blue clay matrix due to local reduction processes, clearly sheared in the fault zone; **g.** weathered brown-orange silt, with small pebbles and locally clayey patches; it turns in a brownish silty clay in the central part of the trench and into a grey-brown clay southward; at the top a distinct paleosoil 10-20 cm thick is locally preserved, **h.** pale brown clayey silt, locally with a red weathered horizon (10 cm thick) at its top; **i.** grey-blue silty clay with coarse sand to fine gravel at its bottom, it turns into

a grey clay southward, some red weathering locally identified at its top; **k.** fine to medium size gravel in grey silty-clay matrix; **m.** brownish silty clay with small pebbles, it represent the distal part of unit *b* (colluvium) and it interfingers with unit *n* southward; **n.** brownish clay, with several small roots from the grass above, the development of a soil horizon is probably not permitted by frequent overflooding of the nearby channel; **p.** dark black-brown clay, it becomes dark grey northward; **q/q2.** dark brown to dark greyish purple clay with a small amount of silt increasing northward, it turns into a grey-brown clay to the south; **r.** dark grey clay, with patches of whitish clay at the bottom; **s.** black sandy silt, coarser at the bottom, with wood and plants concentrated in the upper part, ends abruptly northward; **t.** brown gravel, coarser to the south, ends abruptly northward.

Figure 9. (A) View of the Cinarli trench from the south, notice the low energy organic deposits ponding against the main scarp offset by the fault zone B (see fig. 8C); rectangle encloses the location of the ^{210}Pb sampling; **(B)** Detail of the ^{210}Pb sampling location; **(C)** Summary of results for ^{210}Pb dating.

Figure 10. Left: map view of the fault scarps, of the trace of the topographic profiles and of the AKSU trench location (surveyed by total station); right: topographic profiles across the main and antithetic scarps. 1999 throws and cumulated scarp heights are shown too (black and gray, respectively).

Figure 11. (A) Simplified log of the west wall of the AKSU trench. Stars indicate event horizons, triangles are radiocarbon sample locations (details in Table 1); hexagon shows the location of the glass fragment. Stratigraphy: **a.** silty light brown active soil

with roots; **b.** dark silt with pebbles at the bottom (base of ploughed zone); **c.** U-shaped crumbly brownish silt with pebbles (root zones of big dead trees) only in the southern part of the trench; **d.** light brown mud with sparse pebbles; **e.** brown silt with sparse pebbles; **f.** pebbles, cobbles and small granules in a clayey silty matrix, wedge shaped deposit interfingering with unit *e* (scarp-derived colluvium); **g.** brown silty clay with rare pebbles; **h.** yellowish brown silt with rare pebbles, more clayey in the upper part; **i.** dark brown silt with pebbles (up to 4 cm in diameter); **m.** brownish silt with pebbles (only in the fault zone); **n.** yellow silt only on top of unit p, 10 to 20 cm thick, top eroded toward the fault zone; **p.** alluvial fan: sandy silt with cobbles and pebbles, locally lens of fine gravel, coarse sand and boulders (light colour). **(B)** View of the trench site from north. **(C)** View of the antithetic fault zone in the west wall. **(D)** Glass fragment found in the lower part of unit e (hexagon in panel A).

Figure 12. Correlation of paleoearthquakes along the Düzce fault and inferred age ranges. In the upper panel we report the radiocarbon age probability distribution (dark grey 1σ, light grey 2σ), as well as the ^{210}Pb and the archaeological estimates (rectangles, small letters indicate the stratigraphic unit for which the ^{210}Pb refer to), used to set the age of an event horizon in each trench. Black arrows indicate whether the sample pre-dates or post-dates the event. Dashed black lines indicate a preferred age for the event given the stratigraphic considerations discussed in the text. Names of the events are indicated and are the same used in the logs (figures 4 to 11) and in Table 2. In the middle panel we show the correlations among trenches, in most cases events are correlated between trenches on the basis of their age compatibility and local sequence of the events. Grey horizontal lines represent the best age range of events on the basis of radiocarbon dating and assuming that the penultimate earthquake occurred before

AD1900. Black rectangles (with exception for the 1999 earthquake that is known) show preferred ages of events obtained by including also the other types of dating. Empty rectangle for DUZ5 is indicative of the preferred part of the range obtained on the basis of stratigraphic considerations. Correlated events are renamed as DUZ2 to DUZ5, these represent pre-1999 surface faulting earthquakes that ruptured the same fault extent as in 1999 (see discussion in text). The event horizons from each trench that concurred to the recognition of the correlated events are reported in brackets. In the lower panel historical earthquakes (stars) known to have occurred in proximity of the Düzce fault are reported.

Figure 13.

Integration of paleoseismological results from this work and previous ones. Ellipses show the age range uncertainties for paleoearthquakes, tones of grey indicate different papers. Historical earthquakes are shown too (stars) to complete the frame of available information. Two of the events recognized in this work (DUZ2 and DUZ4) were not recognized before. Recent earthquakes appear to have occurred more closely spaced than previous ones.

Table captions

Table 1.

Measured and dendrochronologically corrected radiocarbon ages of samples collected in the Düzce trenches. Calibration program: Calib Rev 5.02 (Stuiver and Reimer, 2005); calibration dataset from Reimer et al., 2004.

Table 2. Synthesis of paleoearthquakes of the Düzce fault. The first column lists the surface faulting events recognized at each trench. The second column shows the correlation of paleoearthquakes at different locations along the fault naming them DUZ1 to DUZ5, where DUZ1 is the 1999 earthquake. In column three the age interval of occurrence of the event is given based both on radiocarbon, ^{210}Pb dating (indicated with *), or archaeological evaluations (indicated with **). In column four we attributed an arbitrary confidence level based on the constraints existing on the recognition of the event itself.

Table 1

lab #	sample	Rad. Age BP	δ13C	CALIBRATION	PROB 0.95 (2 sigma)	Type of material
Poz-13745	KW-45	modern	-27.4			charcoal
Poz-13711	KW-02	335±30	-29.8	AD 1475-1640	1.000	charcoal
Beta 201526	KW-20	890±40	-25.5	AD 1035-1220	1.000	wood
Beta 201525	KE-08	1220±40	-23.3	AD 685-890	1.000	charcoal
KIA 22286	MAN1-W21	375±25	-23.97	AD 1445-1525 AD 1560-1565 AD1570-1630	0.655; 0.012; 0.334	charcoal
KIA 22285	MAN5-W20	297±27	-26.79	AD 1495-1600 AD 1615-1655	0.717; 0.283	charcoal
KIA 22293	MAN5-W16	801±27	-30.23	AD 1185-1200 AD 1205-1275	0.038; 0.962	charcoal
KIA 22296	MAN5-W13	1317±37	-25.59	AD 650-770	1.000	charcoal
KIA 22295	MAN1-W23	36±24	-22.87	AD 1700-1725 AD 1815-1835 AD 1880-1915 AD 1950-1955*	0.131; 0.088; 0.618; 0.164	charcoal
KIA 22288	MAN6-W18	modern	-34.79	----	----	charcoal
KIA 22287	MAN6-W11	85±35	-22.53	AD 1685-1735 AD 1805-1930 AD 1950-1955*	0.274; 0.713; 0.013	charcoal
KIA 22290	MAN6-E35	200±25	-26.51	AD 1650-1685 AD 1735-1805 AD 1930-1950	0.261; 0.564; 0.175	charcoal
KIA 22291	MAN6-E37	123±20	-25.97	AD 1680-1740 AD 1755-1760 AD 1800-1895 AD 1905-1935 AD 1950-1955	0.290; 0.017; 0.541; 0.151; 0.002	charcoal
Beta 195101	CH-W01	60±50	-24.5	AD 1680-1740 AD 1750-1760 AD1800-1940 AD 1950-1955*	0.266; 0.013; 0.698; 0.023	wood
Beta 201522	CH-W02	240±60	-25.6	AD 1480-1700 AD 1720-1820 AD 1830-1880 AD 1920-1950	0.573; 0.294; 0.038; 0.095	wood
Beta 201523	CH-W07	300±40	-25.3	AD 1475-1660	1.000	charcoal
Beta 195103	CIN1-W500	630±60	-26.9	AD 1280-1420	1.000	wood
Beta 195102	CIN1-W310	980±40	-27.1	AD 990-1155	1.000	wood
KIA 22294	CIN1-W16	112±42	-30.85	AD 1675-1770 AD 1770-1775 AD 1800-1940 AD1950-1955	0.343; 0.010; 0.638; 0.008	charcoal
KIA 22292	CIN1-W03	690±28	-25.59	AD 1270-1310 AD 1360-1385	0.736; 0.264	charcoal
Beta 201519	AK-W06	1080±40	-25.1	AD 890-1020	1.000	charcoal
Beta 201520	AK-W29	140±40	-26.2	AD 1670-1780 AD 1795-1895 AD 1905-1955	0.448; 0.380; 0.172	charcoal

1955* or 1960* denote influence of nuclear testing C-14

Table 2

Trench KAY 40.776095, 31.313858 (WGS8	***Earthquake Correlation***	***Age interval***	***Confidence***
Most recent (KAY-1)	DUZ-1	AD 1999	100%
penultimate (KAY-2)	DUZ-2/3	after AD 1475	high
event KAY-3	DUZ-4	AD 1035-1640	medium-high
event KAY-4	DUZ-5	AD 685-1220	medium
Trench MEN6 40.774718, 31.248849 (WGS			
Most recent (MEN6-1)	DUZ-1	AD 1999	100%
penultimate (MEN6-2)	DUZ-2	AD 1685-1930	high
event MEN6-3	DUZ-3	before AD 1685-1930	high
Trench MEN5 40.774660, 31.246047 (WGS8			
Most recent (MEN5-1)	DUZ-1	AD 1999	100%
penultimate (MEN5-2)	DUZ-3	AD1495-1950	medium
event MEN5-old	DUZ-4	AD1185-1655	medium
Trench MEN1 40.774660, 31.246047 (WGS8			
Most recent (MEN1-1)	DUZ-1	AD 1999	100%
penultimate (MEN1-2)	DUZ-2	AD 1700-1950 *[possibly close to AD1880*]*	medium-high
event MEN1-3	DUZ-3	AD 1445-1950	medium
Trench CH 40.766222, 31.131424 (WGS8			
Most recent (CH-1)	DUZ-1	AD 1999	100%
penultimate (CH-2)	DUZ-2	AD 1680-1950	medium
event CH-3	DUZ-3	AD 1680-1950	medium-high
Trench CIN 40.765541, 31.111827 (WGS			
Most recent (CIN-1)	DUZ-1	AD 1999	100%
penultimate (CIN-2)	DUZ-2	AD 1675-1900 *[possibly close to AD1900*]*	medium-high
event CIN-3	DUZ-3	AD 1280-1700 *[possibly close to AD1700*]*	medium-high
Trench AKSU 40.7569, 30.9562 (WGS84)			
Most recent (AKSU-1)	DUZ-1	AD 1999	100%
penultimate (AKSU-2)	DUZ-2	after AD 1670-1950, shortly before AD 1880-1940**	high
event AKSU-3	DUZ-5	close to or right before AD 890-1020	low

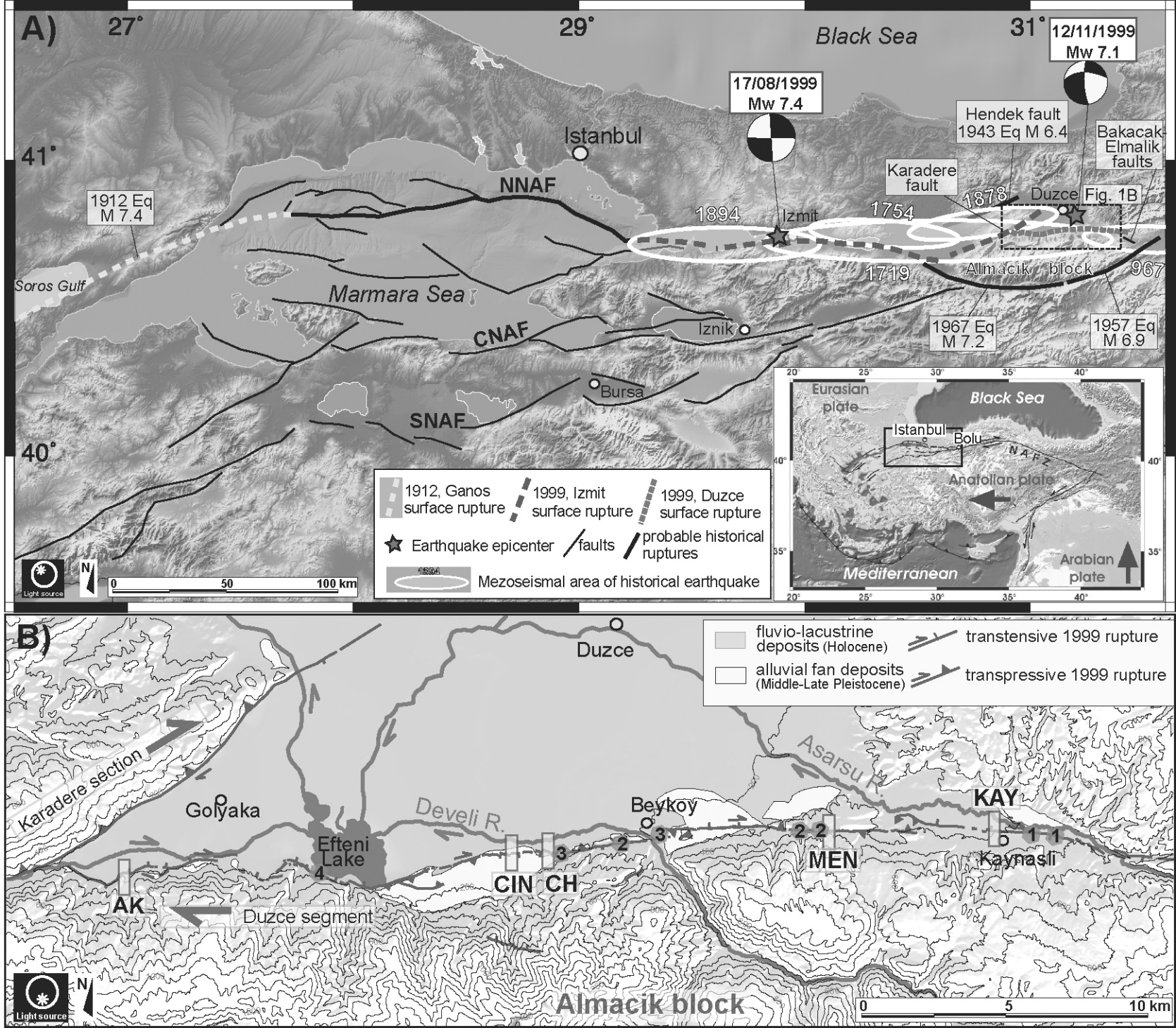
A)
27°
29°
31°
41°
40°
Black Sea
12/11/1999
Mw 7.1
17/08/1999
Mw 7.4
Istanbul
Hendek fault
1943 Eq M 6.4
Bakacak-
Elmalik
faults
Karadere
fault
1878
Duzce
Fig. 1B
NNAF
1912 Eq
M 7.4
1894
Izmit
1754
1719
Almacik block
967
Soros Gulf
Marmara Sea
CNAF
Iznik
1967 Eq
M 7.2
1957 Eq
M 6.9
Bursa
SNAF
Eurasian
plate
Black Sea
Istanbul
Bolu
NAFZ
Anatolian plate
Mediterranean
Arabian
plate
1912, Ganos
surface rupture
1999, Izmit
surface rupture
1999, Duzce
surface rupture
Earthquake epicenter
faults
probable historical
ruptures
Mezoseismal area of historical earthquake
Light source
N
0
50
100 km
B)
Duzce
fluvio-lacustrine
deposits (Holocene)
alluvial fan deposits
(Middle-Late Pleistocene)
transtensive 1999 rupture
transpressive 1999 rupture
Karadere section
Golyaka
Develi R.
Asarsu R.
Beykoy
KAY
Efteni
Lake
CIN
CH
MEN
Kaynasli
AK
Duzce segment
Almacik block
Light source
N
0
5
10 km

Fig. 1

A) Kaynasly trench - west wall

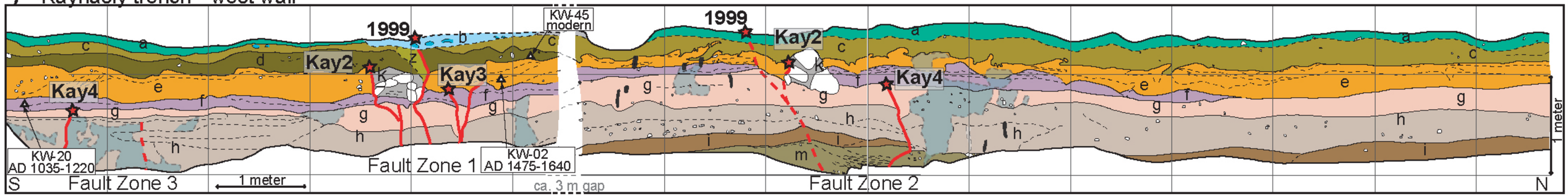

Kaynasly trench - east wall (mirror image)

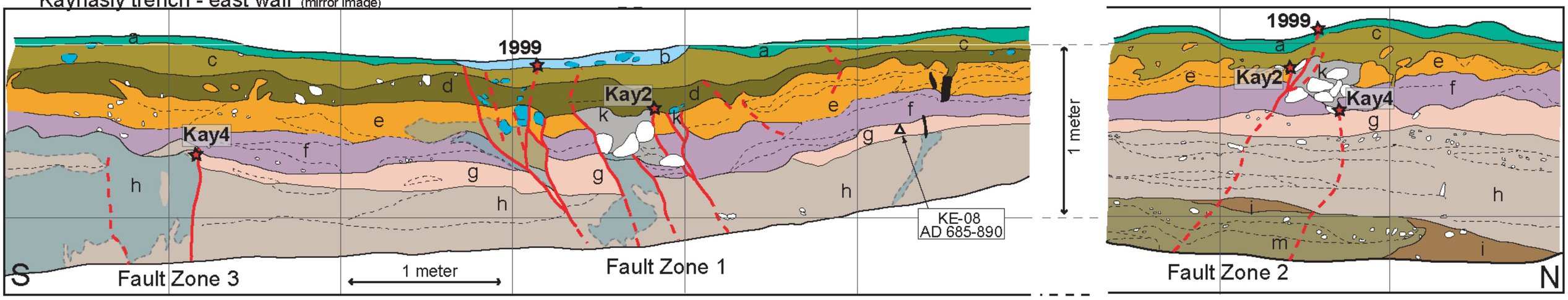

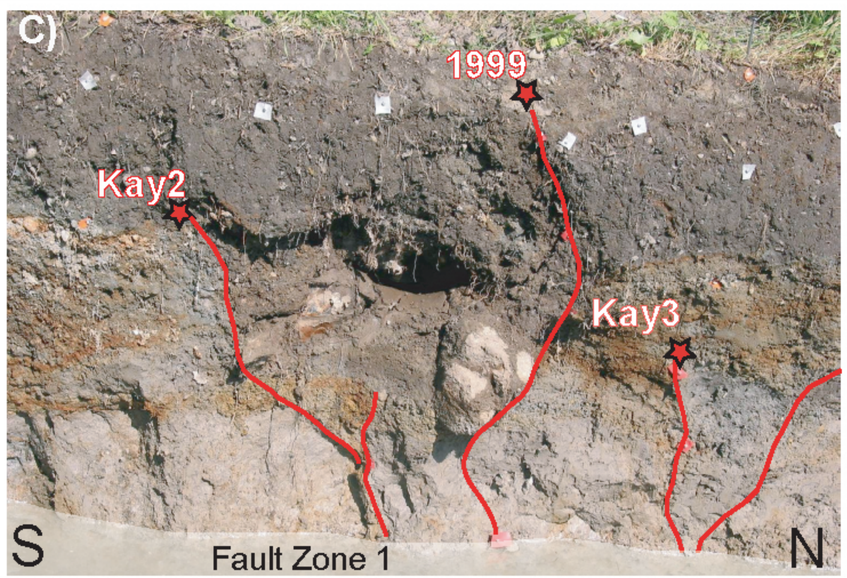

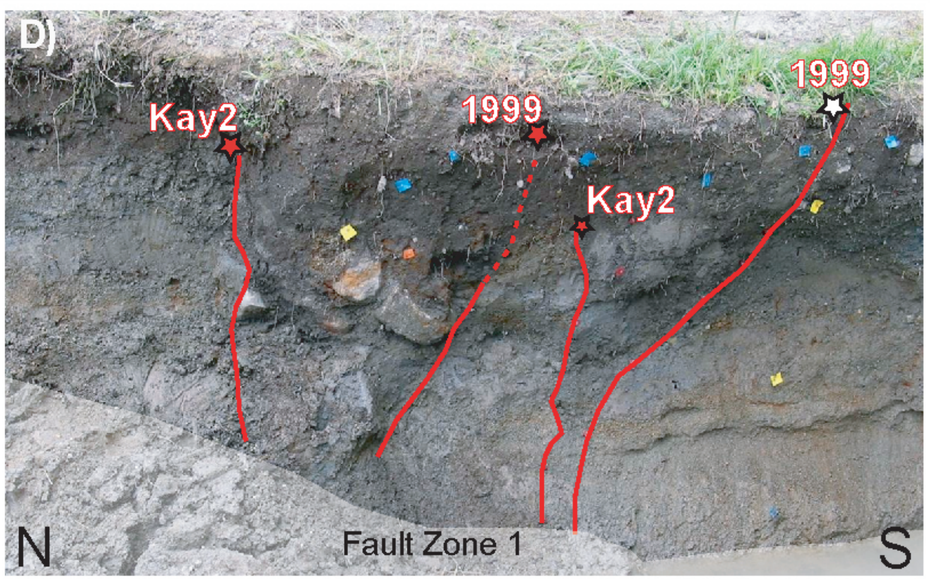

Fig. 2